BACHELOR

Surfactant spreading in liquid-liquid systems

Wong, C.H.

Award date:
2012

Eindhoven University of Technology
Department of Applied Physics
Group Mesoscopic Transport Phenomena

Bachelor Project

Surfactant spreading in liquid-liquid systems

Author: Chun Hou Wong
Supervisors: Dipl. Ing. D.K.N. Sinz & Prof. Dr. A.A. Darhuber

August 22, 2012

1 Summary

The surfactant transport through induced Marangoni flow along discontinuous liquid-liquid interfaces is dependant on geometrical parameters and the type of surfactant. Existing studies and literature are mainly focused on spreading along liquid-air interfaces but the spreading along continuous liquid-liquid interfaces was studied by S. Berg[5]. However Sinz[6] recently described the spreading along discontinuous interfaces. The goal of this study was to investigate the effect of geometrical parameters on the spreading as well as the spreading behaviour of different types of surfactants. An increase in cavity height results in a higher surfactant spreading rate. An increase in pattern spacing results in a lower surfactant spreading rate. Specific combinations of surfactant and liquid-liquid interfaces can alter the wettability temporarily. The spreading of surfactant along discontinuous interfaces is directly relevant to enhanced oil recovery. In oil recovery, surfactant induced Marangoni flows offer an efficient way of achieving flow in dead end pores or heavily fractured oil reservoirs unreachable by pressure driven flow.

2 Introduction

Crude oil is found in underground oil reservoirs consisting of porous rock formations. A mixture of oil and brine (water+sodium chloride) resides in fractured rock formation and in pores. The pores are either connected pores or dead end pores. The extraction of crude oil is commonly divided in three stages[1]. The primary recovery stage relies on the extraction of oil due to a natural overpressure in the oil reservoir and once this natural driving force is exhausted the secondary methods can be employed to continue oil extraction. The secondary phase relies on external pressure driven flow as these methods involve pressurized injection of water or gas into the oil reservoir. However pressure driven flow based methods are only effective with connected pores but ineffective inside dead end pores and fractured rock because there is a small to no pressure gradient present inside dead end pores and fractured rock. Tertiary methods or also known as enhanced oil recovery methods, refer to techniques such as thermal, biological or chemical injection methods. The commonly used chemical injection method is the flooding of the oil reservoir with surfactants. Surfactant is an abbreviation of surface active agent. Surfactants lower the interfacial tension between two liquid phases and also induce Marangoni flow. Surfactant based transport mechanisms rely on reducing the interfacial tension of the liquid-liquid interfaces because the surfactants have the disposition to adsorb at these liquid-liquid interfaces. Inside oil reservoirs, surfactants reduce the interfacial tension between the oil and water interfaces. High local concentration of surfactant will cause Marangoni stresses and flow along oil-water interfaces and will give rise to the spreading of surfactant along the oil-water interfaces. Because this transport mechanism is not based on pressure driven flow, surfactants are particularly useful for enhancing the oil extraction inside dead end pores and fractured rock. Although there have been many studies on surfactant spreading along liquid-air interfaces, only one study has been done, by S. Berg[5], on the spreading along liquid-liquid interfaces. However this study was exclusively focused on surfactant spreading along continuous liquid-liquid interfaces. Nonetheless the conditions inside oil reservoirs do not dictate the sole presence of continuous interfaces but also the possibility of discontinuous interfaces. The formation of discontinuous oil/water interfaces depends on different factors but the wettability of the rock surface plays a major role. Inside oil reservoirs there are three main types of rock surface wettability:'oil-wet, water-wet and mixed-wet'. These three possible wetting scenarios are shown in figure 1. Oil and water wet refer to the condition in which the rock matrix, i.e. the oil containing pores are respectively predominantly wetting for the oil or water phase. Furthermore mixed wettability is the condition where both wetting properties are found and mixed wettability accommodates discontinuous interfaces.

In this study the discontinuous interfaces are implemented experimentally through a chemical patterning procedure to confine aqueous liquids to specific locations inside an oil bulkphase. Chemically patterned glass substrates are used to confine the liquid phase(polar) and the oil bulkphase(apolar) in a Hele-Shaw-cell type of geometry. This study focuses on quantitative measurements of the front edge of the surfactant spreading with different geometrical parameters and different types of surfactant.

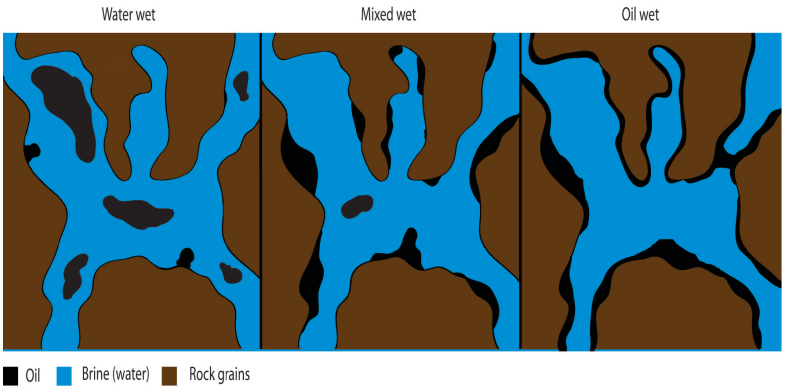

Figure 1: The three possible wettability conditions inside porous rock. Rock that is predominantly wetting for oil or water is called oil wet and water wet respectively. When the rock is for example water wet, water will have a low contact angle. The third condition is called mixed wet where the rock is not predominantly wetting for either water or oil. The mixed wet condition accommodates discontinuous interfaces.

3 Material and methods

3.1 Materials

3.1.1 Surfactants

While there are many types of surfactants, the specific surfactants used in this study are Triton X[2] surfactants. Figure 2 shows the structure of Triton X with an apolar part/chain and 'n' the number of repeating polar chains. Therefore a Triton X surfactant with a larger number 'n' is a more polar or hydrophilic molecule and a lower number 'n' is a more apolar or hydrophobic molecule. The chemical polarity of the surfactants is quantified with the specific HLB values of these surfactants. The HLB[3] value is defined as:

$$HLB = 20 * (M_h/M) \tag{1}$$

Where M_h is the molecular mass of the hydrophilic portion and M is the molecular mass of the entire molecule. This means that a molecule, in this case a surfactant, with a HLB value ranging from 0 to 10 is hydrophobic or oil soluble and a surfactant with a HLB value ranging from 10 to 20 is hydrophilic or water soluble. Three qualitatively different Triton X surfactants were selected based on their HLB value. The selected surfactants: a strongly oil soluble surfactant Triton X-15 with a HLB value of 4.9, a partially oil soluble/partially water soluble surfactant Triton X-45 with HLB value of 9.8 and a Triton X-100 surfactant that is strongly water soluble with a HLB value of 13.4. The surfactant solutions are a dilution of surfactants and dodecane. The surfactant solutions are stained with an Oil Red-O dye for improved visibility of the surfactant propagation during measurements. Solutions with Triton X-100 surfactants are always combined with Triton X-15 to improve the solubility in dodecane.

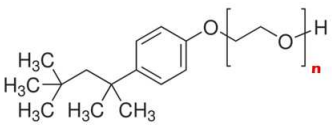

Figure 2: Structural formula of Triton X

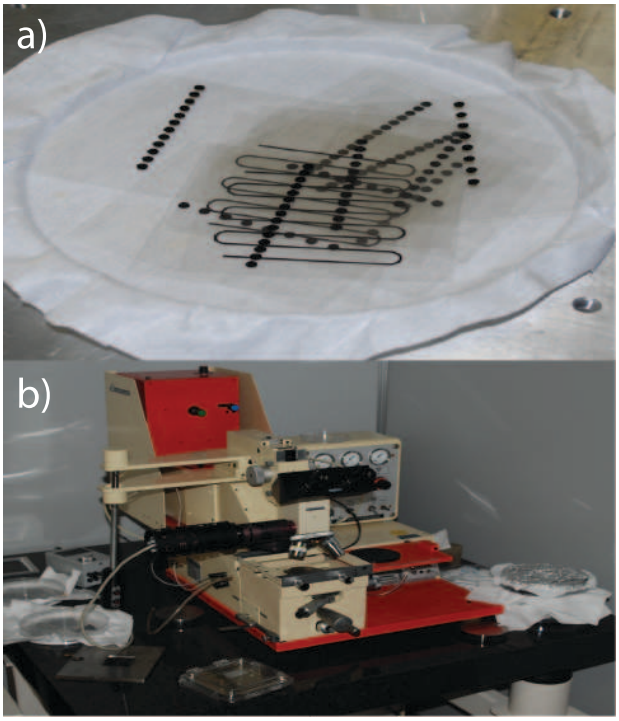

Figure 3: a) Several patternmasks and b) the mask aligner used during the photolithography process.

3.2 Experimental methods

3.2.1 Chemical patterning

A photolithography process is used to fabricate the patterned substrates but prior to the patterning process the glass substrates are put in a potassium hydroxide (KOH) solution and rinsed with de-ionized water afterwards. In the next step the substrates are spin coated with hexamethyldisiloxane (HDMS) at 3000 RPM and with positive photoresist ARP-3510 at 3000 RPM for 40 seconds. This results in a monolayer of HDMS plus a two μm layer of ARP-3510 on the coated side of each substrate. Spincoated substrates are then soft baked at a temperature of 95 degrees Celsius for 60 seconds and put in a sealed container afterwards to avoid UV-light exposure and contaminations. After the cleaning and spincoating process the substrates are then irradiated with UV-light for 15 seconds with a patternmask placed on top of the coated glass. The patternmasks are an aligned row of circles with a variable diameter and with a variable gap spacing. After the UV irradiation process the photoresist pattern is developed by submerging the substrates in a 1:1 developer solution of AR300-35 and de-ionized water. Unmasked coating of HDMS and ARP-3510 are dissolved in the developer solution. Afterwards the processed substrates are rinsed with de-ionized water and put through a ozone cleaning for 2 to 3 minutes. To make the uncovered regions hydrophobic, the substrates are processed with droplets of perfluorooctyl-trichlorosilane (PFOTS) which are deposited inside a container with the developed substrates and heated at 100 degrees Celsius. The deposited PFOTS droplets evaporate inside the sealed container and result in a heterogeneous wettability pattern on the glass substrates. After rinsing the substrates with acetone, the photoresist is removed and this reveals the surface pattern. The diameter and gap spacing of the hydrophilic circles depends on the patternmask used during the process. The process proceeds with rinsing the samples with acetone and de-ionized water. The glass pairs are stored and cleaned in a (pure) sulfuric acid solution before and after any experiment. Figure 3 shows, a) the collection of pattern masks and b) the mask aligner.

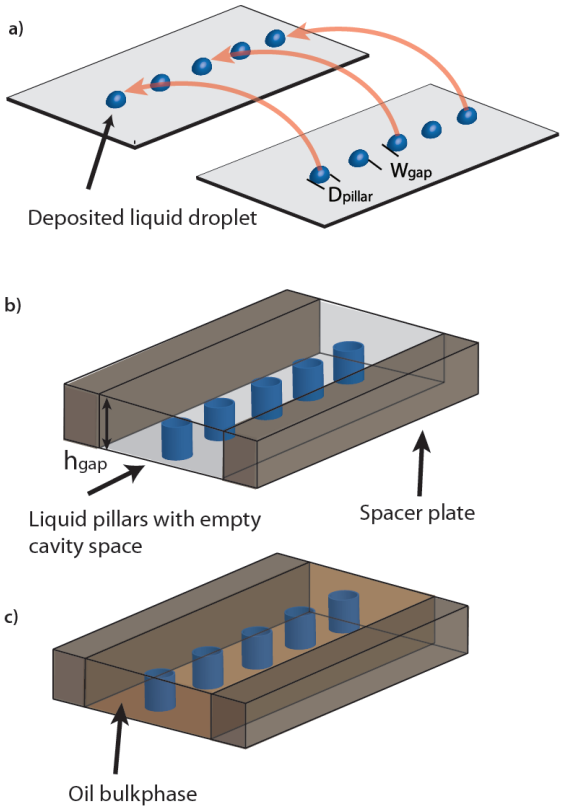

Figure 4: Experimental procedure to fabricate the liquid pillar geometry.
a) The liquid deposition onto the hydrophilic circles on each coated substrate side. The hydrophilic circles have identical gap spacing W_{gap} and an identical diameter D_p. De-ionized water or ethylene glycol is used to form the liquid pillars.
b) To create the cavity space, the glass substrates with the aligned row of deposited liquid are stacked together with two spacer plates between the glass substrates on two sides. Afterwards the glassplates are fixed together with steel clamps.
c) The oil bulkphase is added into one side of the cavity space until the cavity is filled entirely. Dodecane is used as the oil bulkphase in this study.

3.2.2 Sample preparation

Liquid is deposited on the hydrophilic circles on a pair of patterned glass substrates. In this study the deposited liquid is either de-ionized water or ethylene glycol. Using water is more realistic because water is naturally present in the porous rock formations and also some oil extraction methods use water floods. Although ethylene glycol is not present in oil reservoirs, the sample preparation with ethylene glycol is easier due to a lower evaporation rate. After the liquid deposition, the drops on the hydrophilic circles are aligned and stacked on top of each other as sketched in fig4. The resulting cavity space between the two glass substrates is filled with a continuous dodecane oil bulkphase. Upon contact, the droplets on the top & bottom substrates merge and form liquid pillars. The height of the pillars depends on the thickness of the spacers plates. The glass substrates and spacer plates are fixed together using steel clamps. The entire construction is positioned between the camera and lightsource.

3.2.3 Experimental setup

Figure 6 shows the setup for measuring the surfactant propagation front edge. A Pike F145B camera is used for imaging the surfactant spreading and the camera is mounted perpendicularly above the sample. A lightsource which provides homogeneous monochromatic (455nm) illumination is positioned below the sample for improved visibility during experiments. An overview of the experimental setup is shown in figure 5 with the different stages of the experimental procedure of a running experiment. Figure 5 a), shows the starting setup for the sample preparation and the situation after the liquid is placed on top of the hydrophilic circles. The volume is calculated before depositing liquid onto the glass substrates, assuming the liquid forms perfect cylinders after alignment. b) The clamps for fixing the sample together are also visible. c) The surfactant is then put into a syringe (or pipette) which shown in. d) The surfactant is deposited into the sample while the mounted camera records the experiment.

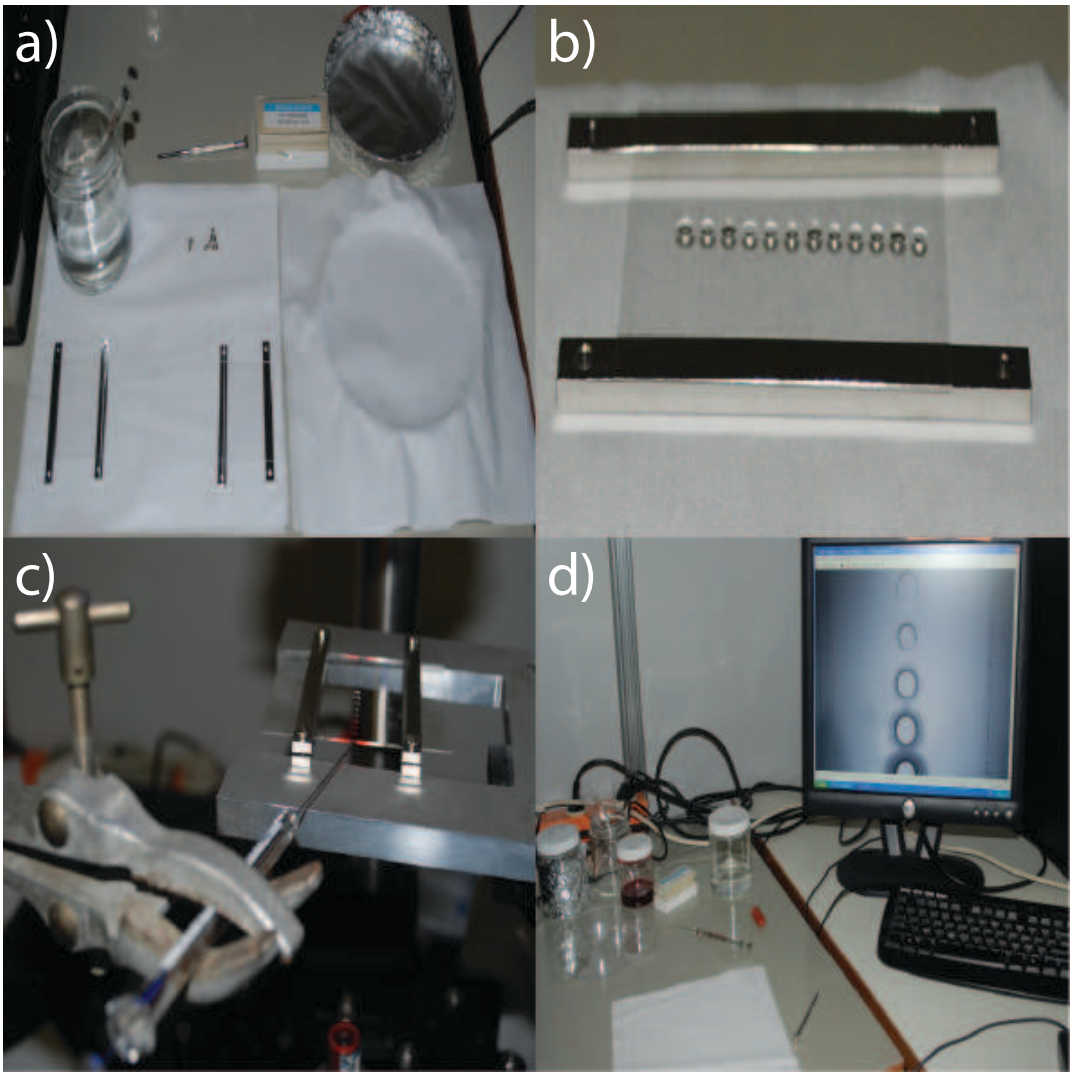

Figure 5: The different stages of the experimental procedure: sample preparation, surfactant deposition and recording during an experiment

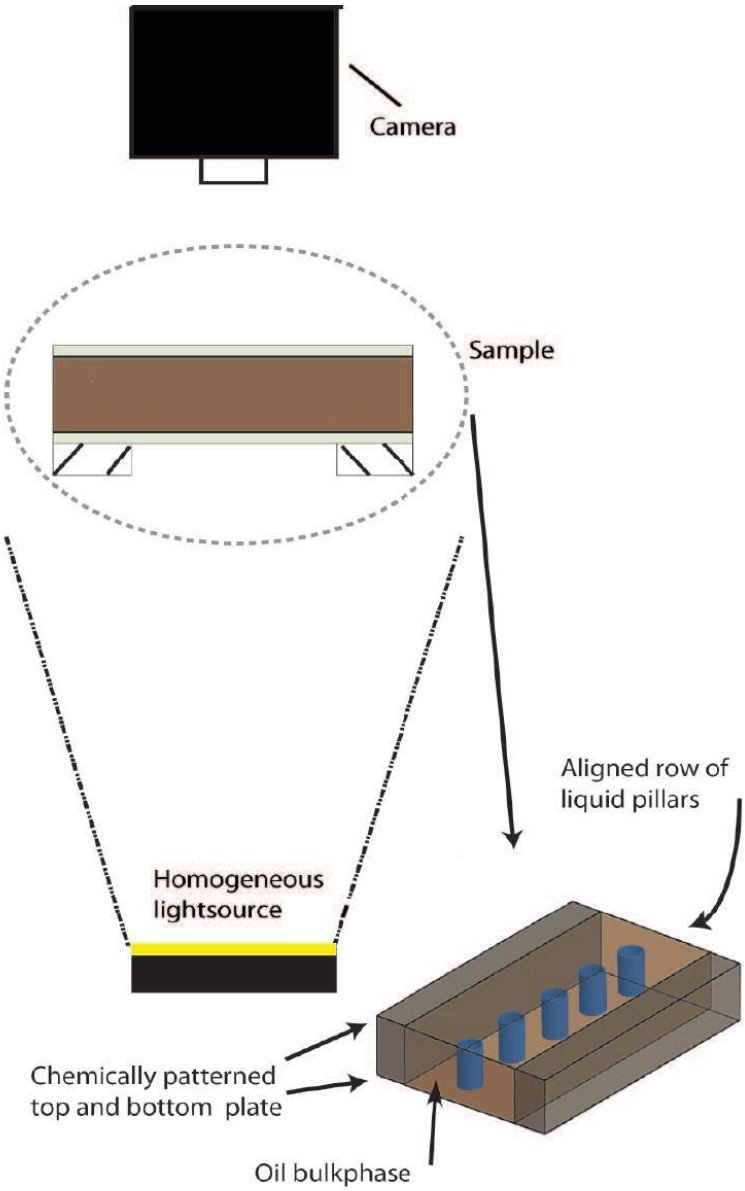

Figure 6: A sketch showing the side view of the experimental setup. The sample is positioned between the camera (above) and the lightsource (underneath). Diffuser plates are attached to the lightsource to homogenise the illumination. A detailed depiction of the sample configuration on the bottom and the top are two chemically patterned glass plates with a hydrophobic surface and a row of hydrophilic spots. Liquid is deposited on the hydrophilic spots and spacer plates with a thickness of h_{pillar} are placed between the glassplates at each side. This results in a cavity between the glassplates and spacer plates which is filled with a dodecane bulkphase afterwards.

3.3 Marangoni flow

An example of surfactant induced Marangoni flow is shown in figure 7. Surfactant is deposited into the sample with syringes or with pipettes using the capillarity. This will result into local high concentration of surfactant at the deposition area and a decreasing surfactant concentration away from the deposition area. Each time the surfactant reaches a liquid pillar, the surfactant concentration is relatively high at the deposition side compared to the front edge side. The presence of surfactants causes a decrease in interfacial tension at the oil-water interface. As a result the Marangoni stresses induce Marangoni flows along the oil-water interface towards the front edge side and the surfactant spreads around the liquid pillars towards the next pillar.

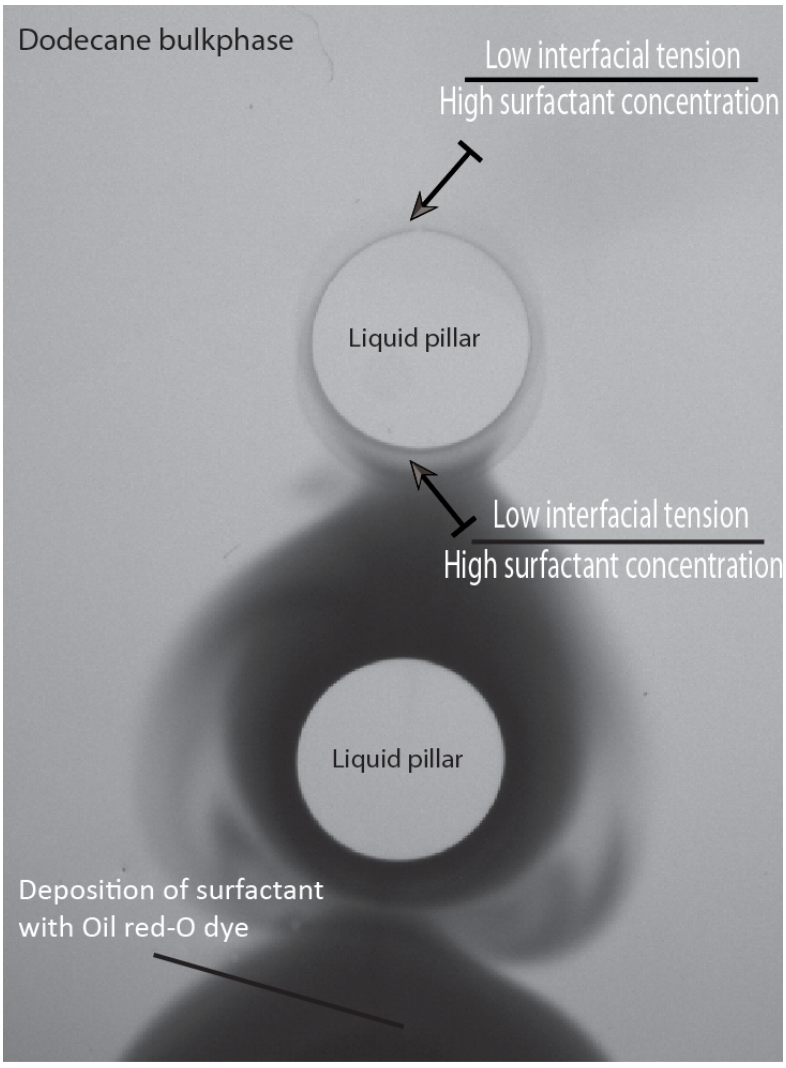

Figure 7: Image captured during an experiment highlighting the Marangoni flow. The surfactant deposition is on the bottom side of the image and will induce Marangoni flow around the affected liquid pillars. This will enhance the surfactant propagation rate to the top side.

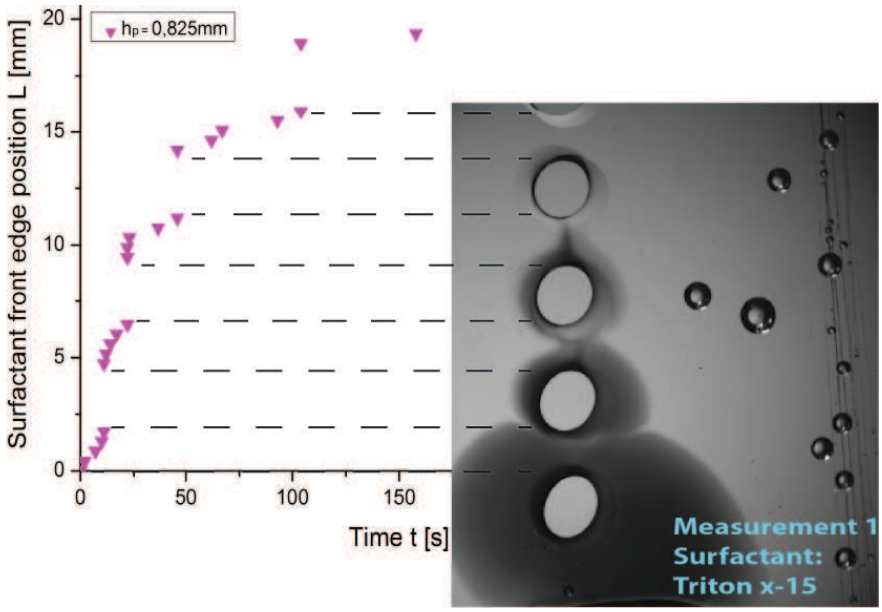

Figure 8: Image showing the measurement procedure. The start position of each measurement is at the 'end' of the first liquid pillar where time $t = 0$ and surfactant front edge position $L = 0$.

4 Results

4.1 Measurements of the surfactant propagation with varied geometrical parameters

4.1.1 Measurements with the variation of cavity spacing

The no-slip condition requires that the fluid velocity at all fluid-solid boundaries is equal to the velocity of the solid boundary. Because of the no slip boundary condition it is expected that a smaller cavity space will translate into a lower velocity field inside the cavity. Measurements were conducted for different pillar height h_{pillar}. The measurement procedure and the starting position of each measurement is shown in figure 8. The first measurements include h_{pillar}: 0.150mm, 0.375mm, 0.600mm, 0.825mm and 1.00mm and the second measurements include h_{pillar}: 0.150mm, 0.375mm, 0.600mm, 0.825mm, 1.00mm and 2.00mm. Figure 10 and figure 11 show the graphs of the measurements with the propagation of the surfactant front edge in mm versus time in seconds. The same surfactant solution is used for each measurement which is comprised of tritonx-15 with a massfraction of 2,1% diluted in dodecane. Existing studies e.g. Berg[5] and Dagan[7], determined that the front edge position L of surfactant spreading scales with time t as L$\sim t^a$. Therefore each individual measurement was fitted with the function: $L = b * t^a$. Coefficient 'a' and 'b' are used to quantify the surfactant spreading rate and these coefficients are shown in figure 14, 15. The initial phase of surfactant spreading is dependent on the deposited surfactant volume. The amount of deposited surfactant in each individual measurement was not proportional to the oil bulk phase volume and the bulkphase volume varies with varying cavity spacing h_p. Consequently the fitting was done after this initial phase.
In experiments for the spreading along the water pillars we frequently observed a pulsed surfactant spreading. This effect has not been studied in detail but has been observed that pulsed surfactant spreading improves the surfactant transport along the liquid pillars. Additionally there is spreading of surfactant away from the center of the water pillar (radial direction) but this is not studied in detail.

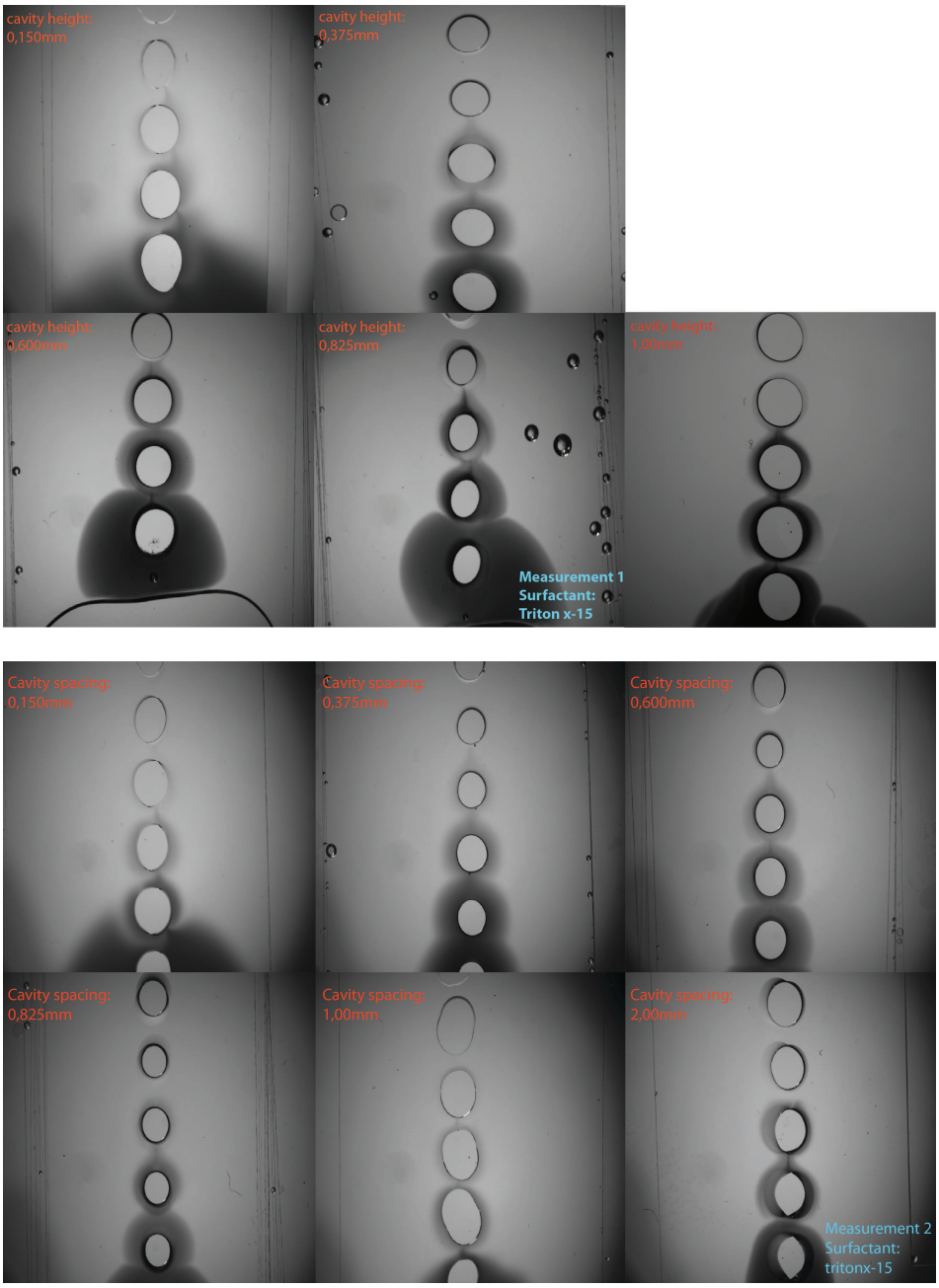

Figure 9: Images showing the leading edge position of the surfactant propagation with varied sample cavity spacing. The top image displays the first measurement with different cavity spacing: 0.150mm, 0.375mm, 0.600mm, 0.825mm and 1.00mm. The bottom image displays the second measurement with the different cavity spacing: 0.150mm, 0.375mm, 0.600mm, 0.825mm, 1.00mm and 2.00mm. The sample consist of a dodecane bulkphase and aligned row of de-ionized water pillars. A dodecane diluted solution of tritonx-15 with a mass fraction of 2.0% is deposited in each sample. This surfactant solution is stained with oil red-O dye and the amount of deposited surfactant solution is 10μL. The liquid pillars show a deformation caused by a non-uniform distribution of surfactant at the liquid pillar interface or caused an excess amount of deposited liquid.

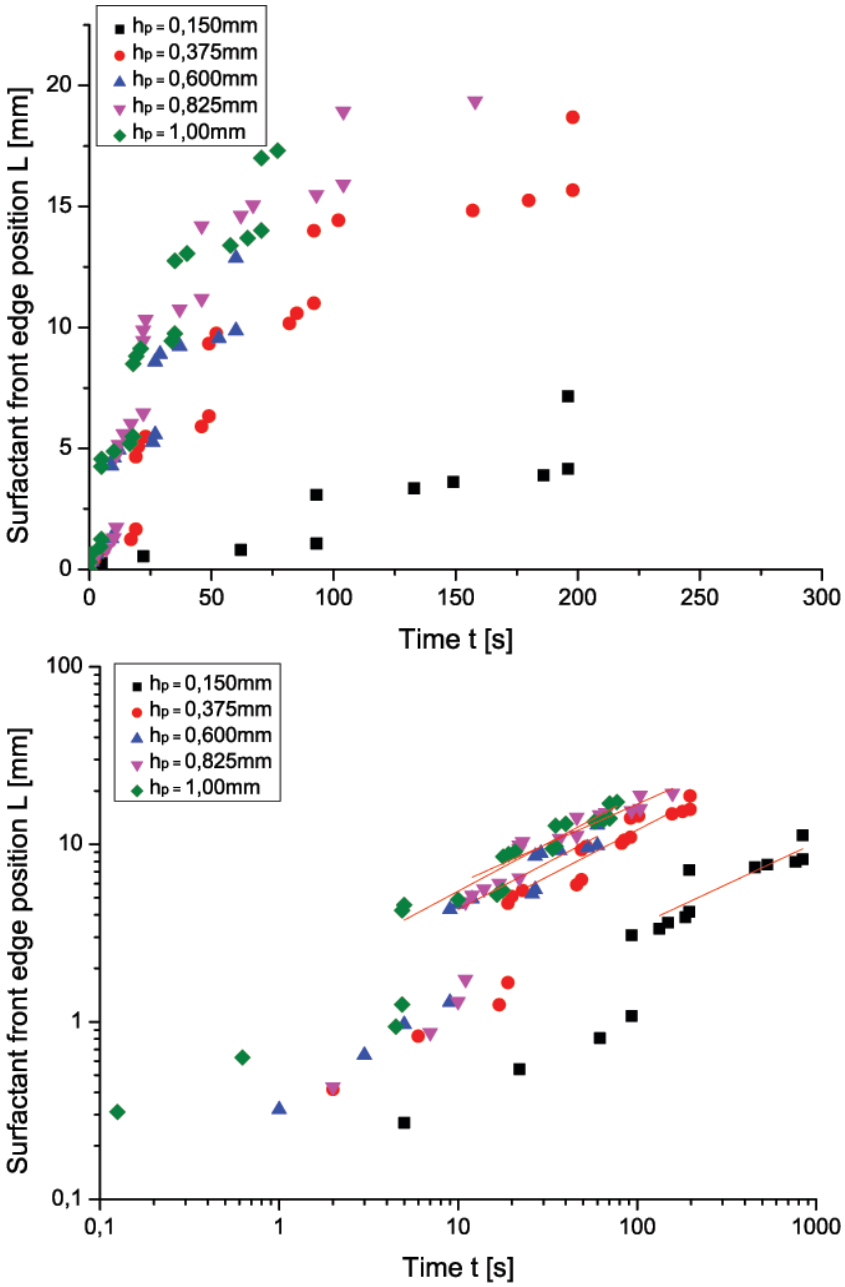

Figure 10: The first series of measurements with varied cavity spacing h_{gap}. At the top, the graph with surfactant position L versus the time t in a linear scale with h_{gap}: 0.150mm, 0.375mm, 0.600mm, 0.825mm and 1.00mm. On the bottom, the graph with surfactant position L versus the time t in a log scale. The measurements are fitted with the fit curve: $L = b * (t^a)$. In these measurements, the sample contains a dodecane bulkphase with (de-ionized) water pillars and a constant gap spacing W_{gap}=3.0mm. Each of the measurements was done with a deposition of 10microliters of surfactant solution with tritonx-15 diluted in dodecane with a massfraction of 2,1%.

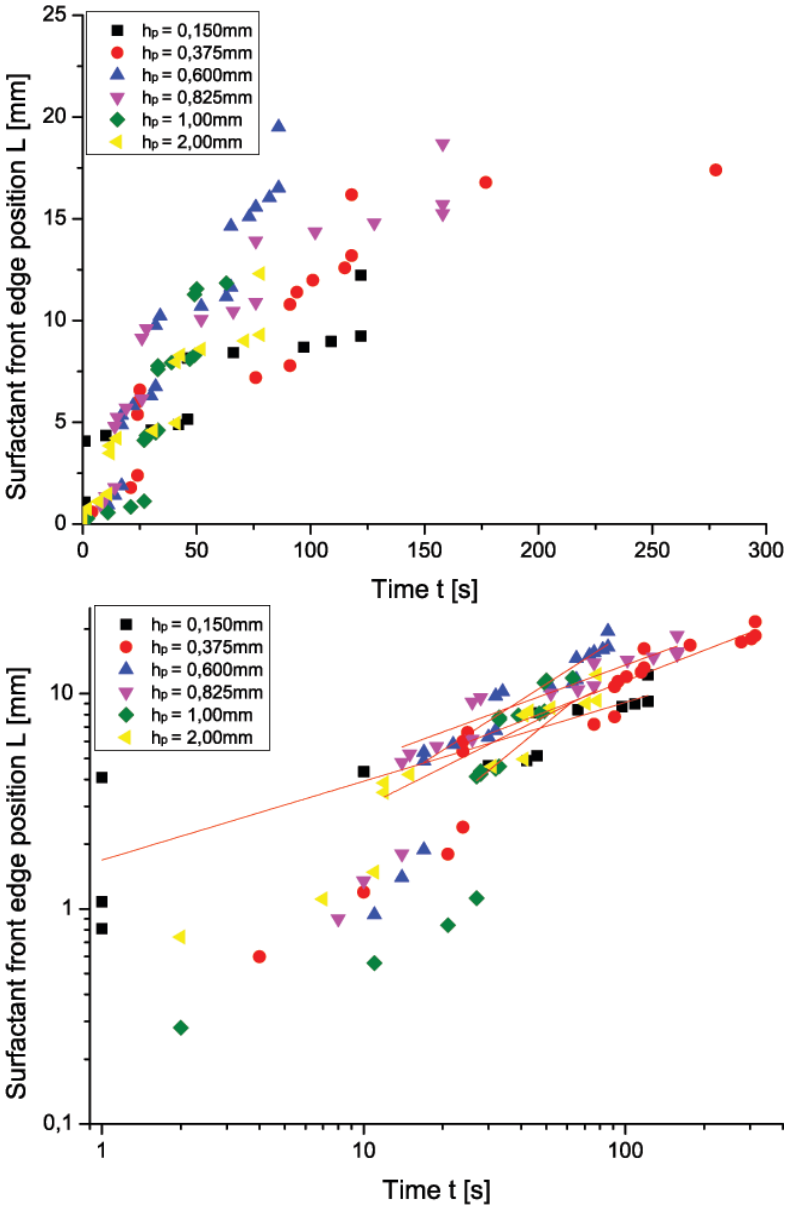

Figure 11: The second series of measurements with varied cavity spacing h_{gap}. At the top, the graph with surfactant position L versus the time t in a linear scale with h_{gap}: 0.150mm, 0.375mm, 0.600mm, 0.825mm, 1.00mm and 2.00mm. On the bottom, the graph with surfactant position L versus the time t in a log log scale. The measurements are fitted with the fit curve: $L = b * (t^a)$. In these measurements, the sample contains a dodecane bulkphase with (de-ionized) water pillars and a constant gap spacing W_{gap}=3.0mm. Each of the measurements was done with a deposition of 10microliters of surfactant solution with tritonx-15 diluted in dodecane with a massfraction of 2.1%. The fit through the measurement with h_{gap}=1.00mm has a coefficient a=1 which can be explained as there was an excess of deposited water. This can be seen in figure 9. As a result, the gap spacing $Wgap$ is no longer constant at 3,0mm but is varying and the L$\sim t^a$ relation between surfactant spreading versus the time is 'altered'.

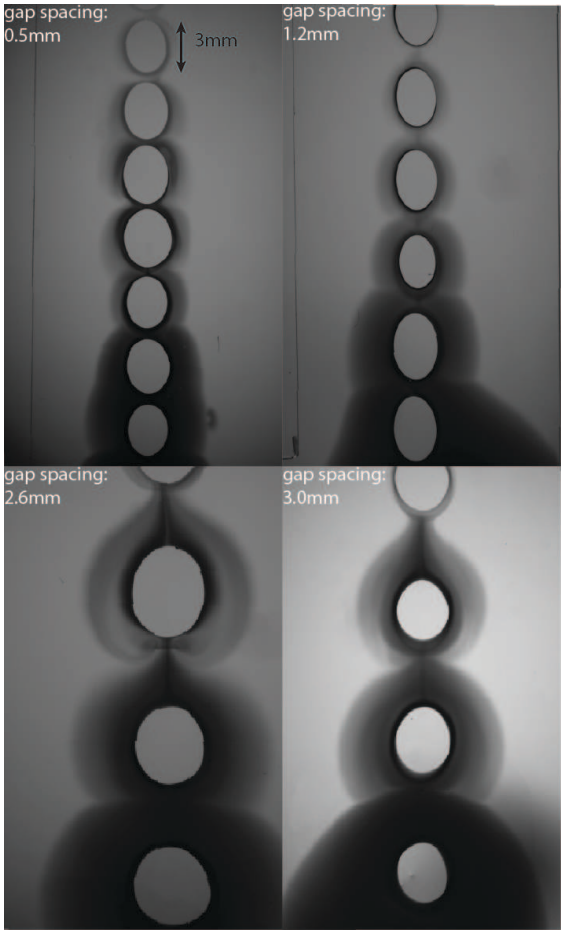

Figure 12: Images showing the leading edge position of the surfactant propagation with varied sample gap spacing. The cavity spacing in each individual measurement is 1.00mm. The sample consist of a dodecane bulkphase and a row of aligned ethylene glycol pillars and a dodecane diluted solution of Triton X-15 with a mass fraction of 2.0% is deposited in each sample. This surfactant solution is stained with Oil Red-O dye and the amount of deposited surfactant solution is 10μL. Because there is a non-uniform distribution of surfactant at the liquid pillar interface that results in the deformation of the pillars or the deformation is due to an excess amount of liquid deposited during the deposition process.

4.1.2 Measurements with the variation of gap spacing

In the measurements with variation of gap spacing the deposited surfactant solution consists of Triton X-15 with 2.0% mass fraction into a dodecane bulkphase with ethylene glycol pillars. Figure 12 shows experiments with the different gap spacings which are 0.5mm, 1.2mm, 2.6mm and 3.0mm. In this study the term gap spacing refers to the distance between each hydrophilic coated circle. The non-uniform distribution of surfactant at the liquid pillar interface causes the pillar to deform. Figure 13 shows the leading front of the surfactant propagation versus the time and the fitted graph with the fitting curve: $L = b * t^a$). The fit coefficients a are shown in figure 14 and the fit coefficients b are shown in figure 15. The velocity of the surfactant spreading with the gap spacing of 0.5mm is $1.47 * (10^{-4})m/s$ which is an order of magnitude (10 times) higher compared to the velocity of propagation in a single phase liquid which is $1.11 * (10^{-5})m/s$, shown in figure 16 with both having a cavity space of 1,0mm. The measurement of the surfactant front edge in the single phase experiment starts after the capillary action has stopped. Speculation: The transport of the surfactant is due to a combination of diffusion and convection through evaporation at the open sides. However figure 17 shows a square root relation between the surfactant front edge position L and time t and this would mean that the transport of surfactant is mainly caused by diffusion as convection caused transport would have a linear relation between L and t instead. This diffusion (and convection) is also present in the liquid-liquid system but the surfactant induced Marangoni flow results in 10 times higher surfactant spreading rate.

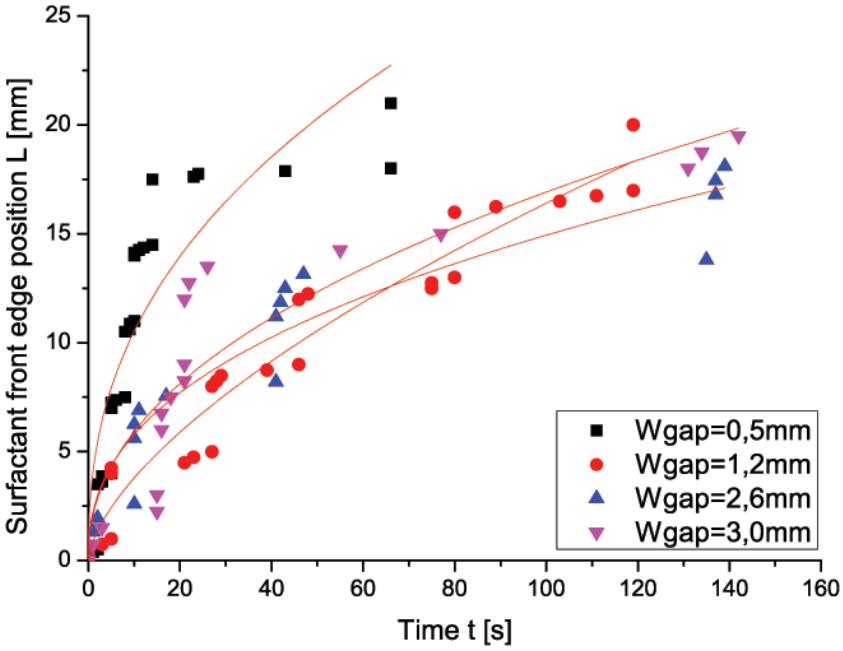

Figure 13: The measurements with varied gap spacing: 0.5mm, 1.2mm, 2.6mm and 3.0mm and fitted with the fitting curve: $L = b * (t^a)$.

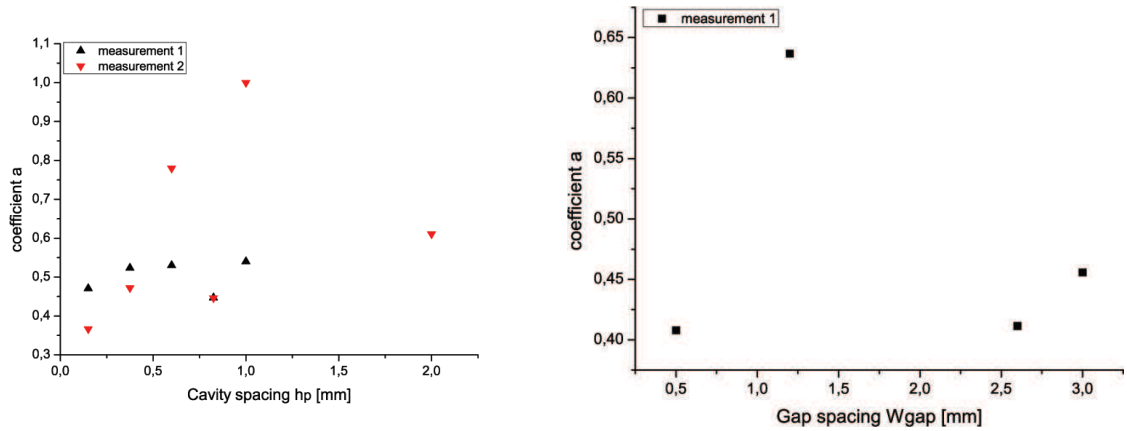

Figure 14: The coefficients a of the measurements with varied cavity spacing and gap spacing, respectively.

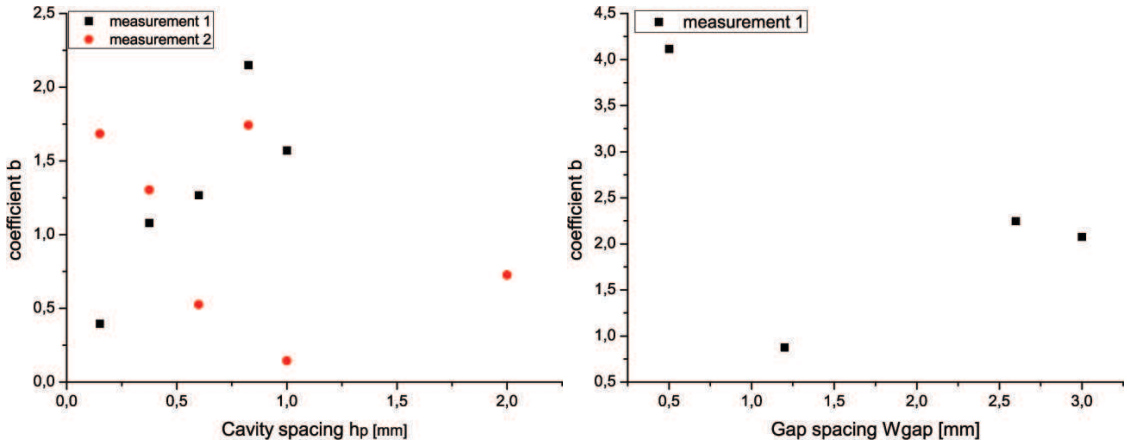

Figure 15: The coefficients b of the measurements with varied cavity spacing and gap spacing, respectively.

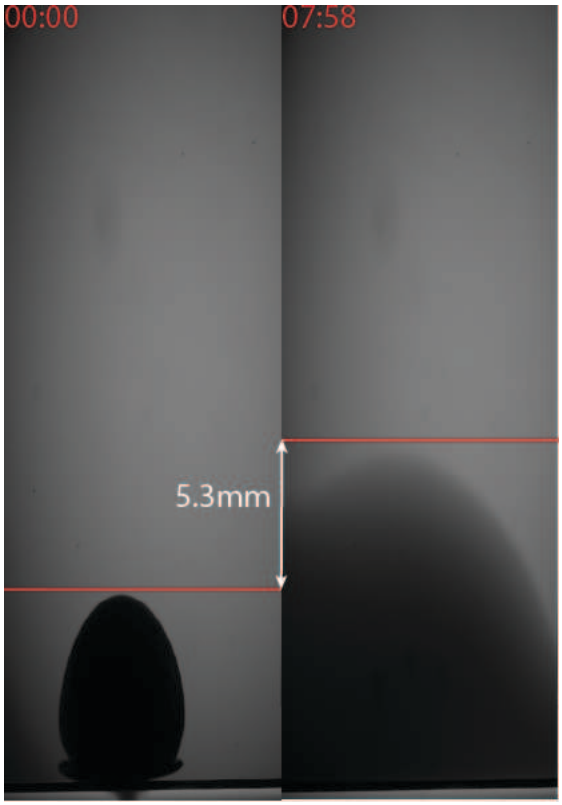

Figure 16: An image showing the surfactant propagation in an one phase dodecane bulkphase with a deposition of Triton X-15 with massfraction of 2.0%.At the start of the deposition until the end of the deposition a distance of 5.3mm has been bridged in a time span of 478 seconds. This amounts to an average front edge velocity of $1.11 * (10^{-5}) m/s$.

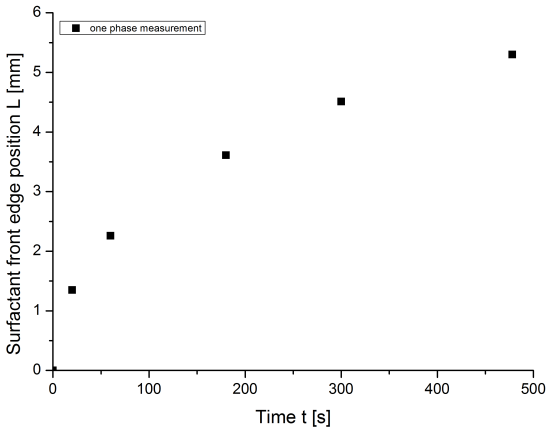

Figure 17: An image showing the graph of the surfactant front edge position L versus time t in the one phase experiment shown in figure 16.

4.2 Wettability Modification

A surfactant solution consisting of Triton X-100 with a massfraction of 0,24% and Triton X-15 with mass fraction of 2.1% is deposited into a dodecane bulkphase with a Hele-Shaw cell geometry. Triton X-100 was mixed together with Triton X-15 to increase the solubility of Triton X-100 in the dodecane bulkphase. The contact between the propagating surfactant and the first water pillar causes the liquid water pillar to break. In addition a funnel was created which ran through the first, second and third water pillar. However this funnel receded afterwards but a layer of water was observed to initially spread out and retract back to the hydrophilic circles to reform the second and third water pillars. This phenomena might be explained with a temporary wettability modification which is only associated with specific combinations of liquid-liquid interfaces and surfactants types. Surfactants have an amphiphilic molecular structure which consists of a hydrophobic part and a hydrophilic part. Triton X-100 surfactants are absorbed by the aqueous phase and cause the liquid pillars to break. It is energetically favorable for Triton X-100 to be adsorbed at the hydrophobic surface of the substrate with the hydrophobic part of Triton X-100 ' pointing inwards' and the hydrophilic part ' pointing outwards'. Speculation: this increases the wettability of the substrate surface and causes the aqueous phase to spread out onto the substrate surface. The aqueous phase starts to retract back to the hydrophilic circles on the substrate due to the desorption back into the aqueous phase as this is energetically favorable. The spreading rate of the aqueous phase is faster compared to the retraction because the adsorption coefficient is larger than the desorption coefficient. This phenomena is shown in figure 18.

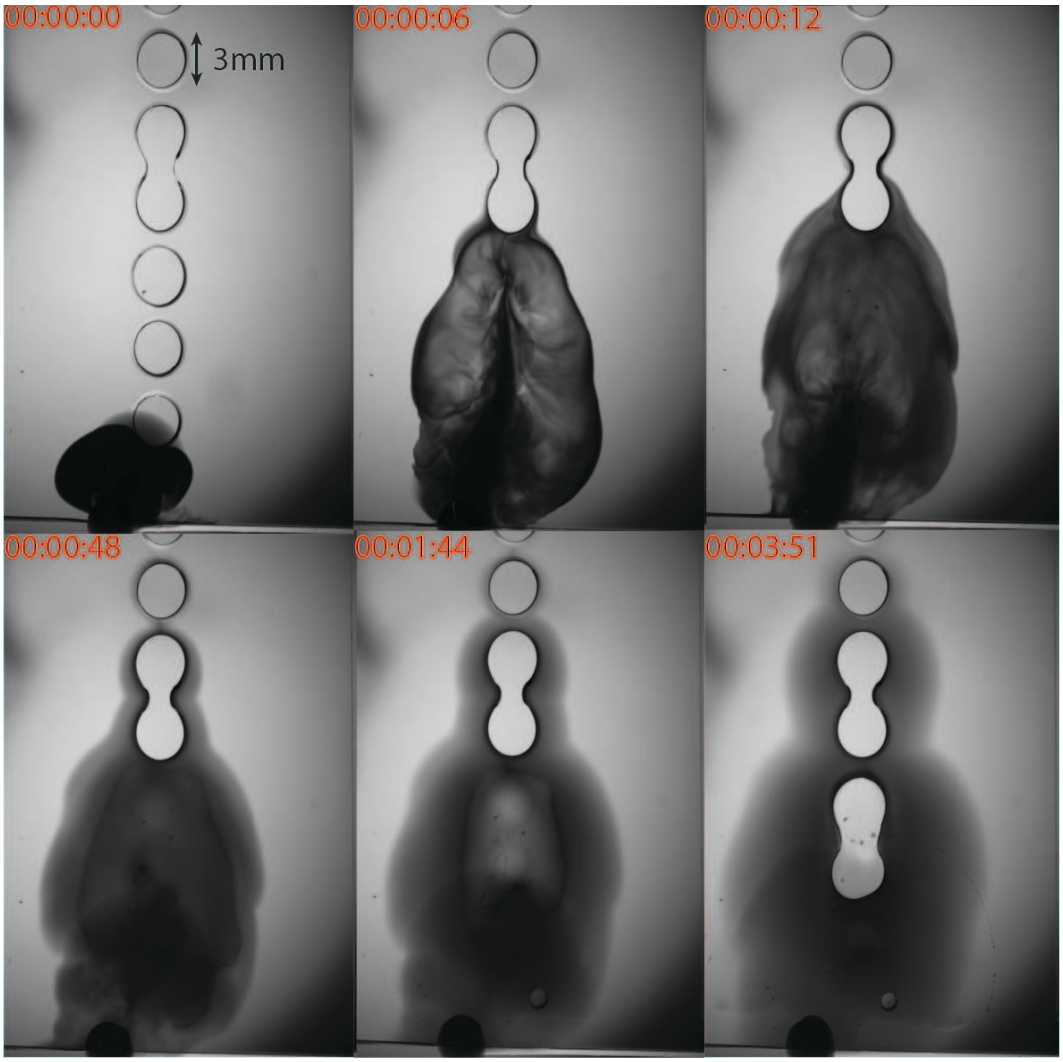

Figure 18: An image with Triton X-100 and Triton X-15 being deposited into a dodecane bulkphase with water pillars. After the surfactant front edge comes in contact with the first pillar, the first, the second and the third water pillars break. The water from these liquid pillars spreads out and retracts after a period of time. The retraction of water will eventually lead to the reformation of the second and third liquid pillars, although with slightly reduced volume. At the start, the water on the third and fourth pillars are merged because of an excess amount of deposited water onto the hydrophilic circles. The incidental deposition on top of the glass substrates explains the contamination at the position of deposition and the black 'ring' that forms after the dye evaporates. The black 'ring' is shown in figure 19

an experiment is shown in figure 20 with the same phenomena but with the sample being a glass cuvette containing one PFOTS coated glass substrate (with no hydrophilic circles). A pure dodecane bulkphase is added and afterwards, a water droplet is deposited onto the PFOTS coated substrate. A syringe containing 10μL of surfactant solution is used to deposit the surfactant solution directly above the water droplet. The surfactant solution is Triton X-100 with a massfraction of 0.28% and Triton X-15 with a mass fraction of 2.1% with Oil Red-O dye and diluted in dodecane. Figure 20 shows the events after the surfactant solution was deposited directly above the water droplet. The surfactant solution causes the aqueous phase to spread out along or close to the bottom surface. The water retracts back to its original position over time.

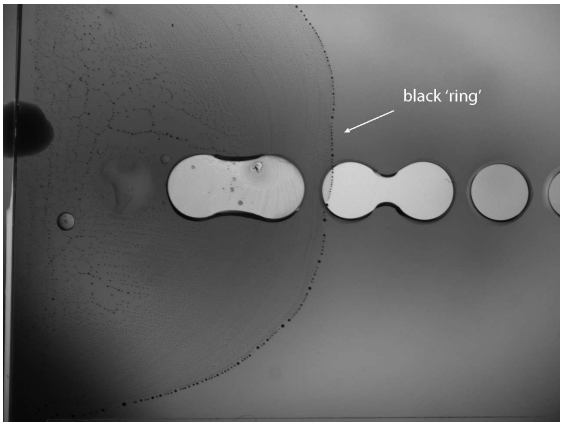

Figure 19: An image highlighting the black ring in figure 18. Speculation: This is evaporated Oil Red-O dye caused by spillage of surfactant solution on top of the sample. which retracts to its original position over time.

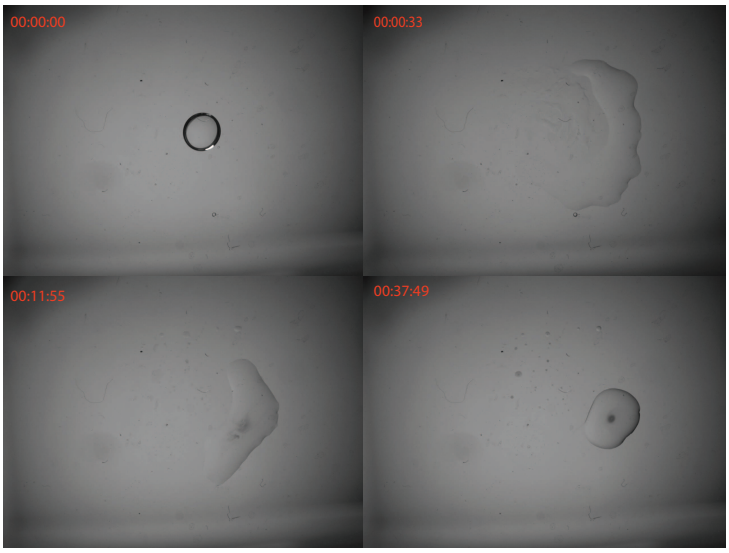

Figure 20: Images showing an expanded water layer after adding a surfactant solution of Triton X-100 and triton X-15 which retracts to its original position over time.

4.3 Miscellaneous observations

This section contains accidental observations which were not studied in detail but these observations would be interesting topics for further research.

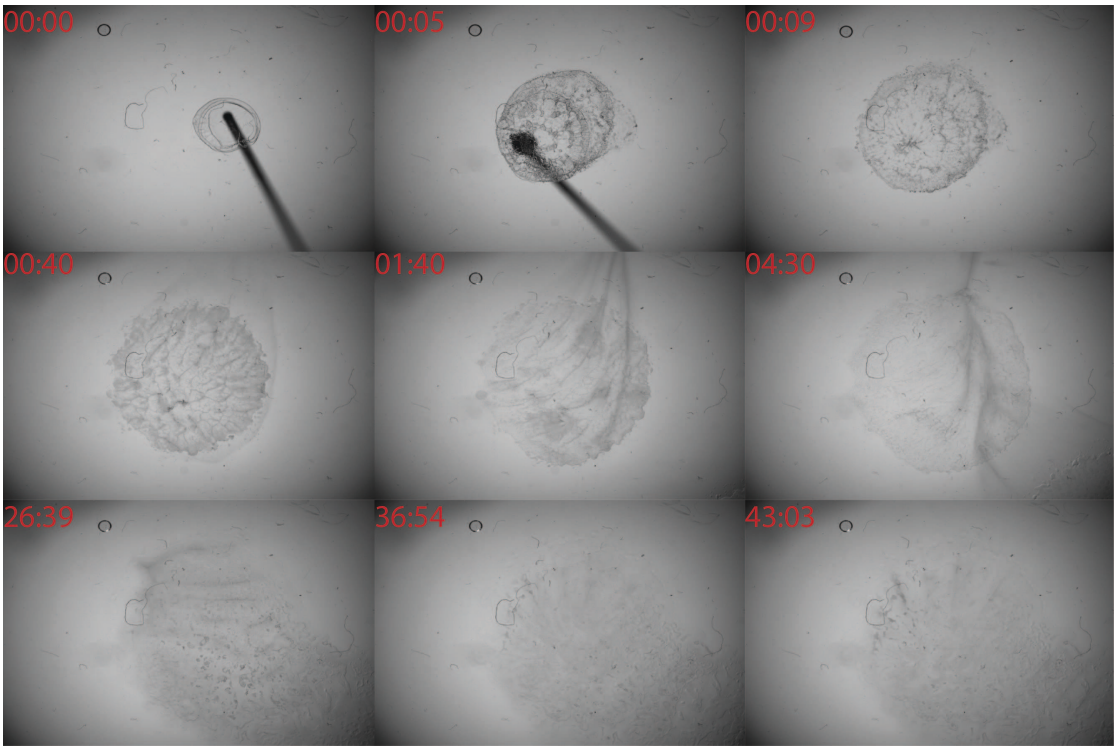

Figure 21: This image shows a glass cuvette containing a surfactant solution of dodecane with Triton X-100 with a massfraction of 0.28% and Triton X-15 with a massfraction of 2,1%. Water droplets are then added into the surfactant solution. The aqueous phase spreads out along the cuvette surface but also to the liquid(surfactant solution)-air interface.

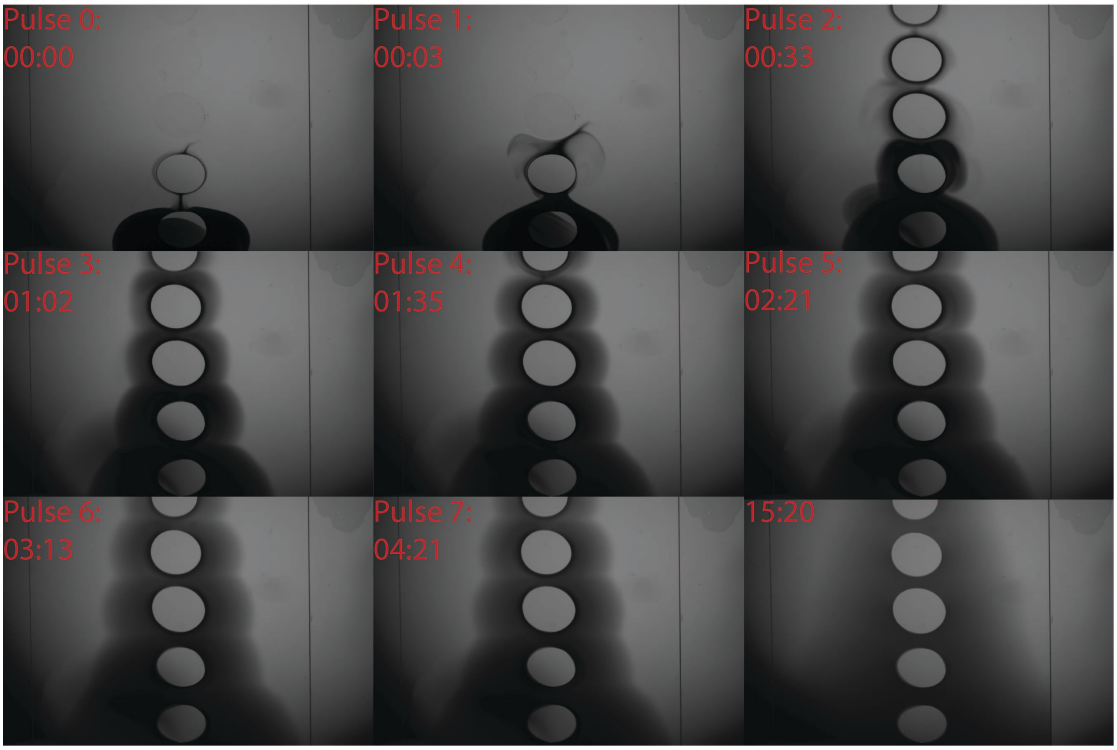

Figure 22: This image shows an experiment where surfactant 'pulses' were observed with a pillar geometry with ethylene glycol pillars immersed into a dodecane bulkphase. The used surfactant was Triton X-15 with a massfraction of 2.1% . The pulses of the second pillar were counted with the initial surfactant contact being defined as Pulse 0. The total number of counted pulses was 7. While using Triton X-15, it was observed that there were more pulses with ethylene glycol pillars compared to water pillars. Speculation: Triton X-15 has a HLB value around 5 which makes it oil soluble or hydrophobic. Even though Triton X-15 is hydrophobic, ethylene glycol is relatively less polar than water and this makes Triton X-15 'more soluble' in ethylene glycol. This might explain the difference in the number of pulses between ethylene glycol and water. Even though this was not studied in detail, hypothesis: more pulses will increase the surfactant spreading along the liquid pillars.

5 Conclusions

The surfactant spreading rate is dependant on geometrical parameters such as the cavity spacing and gap spacing. The results indicate an increase in the surfactant propagation rate with a larger cavity spacing. Moreover the variation of gap spacing between discontinuous water interfaces also has an effect on the propagation rate. A smaller gap spacing between the discontinuous water interfaces results in a faster surfactant propagation rate. The surfactant spreading rate is also dependant on the type of surfactant. Although the used Triton X surfactants are in some extent soluble in water but only Triton X-100+Triton X-15 caused the water pillars to break and reform after a period of time.

6 Appendix

6.1 Surfactant deposition

The problem with the surfactant deposition is the appropriate amount of deposited surfactant during the experiments. The main issue is the method of deposition which is either using a syringe or an ordinary glass pipette. The syringe has a limited capacity with the max capacity of 10μL and the pipette has a sufficient capacity but the deposition is done manually and by eye without any accurate equipment. Moreover, the same amount was deposited with each of the varied cavity spacing measurements although the ratio of surfactant and oil bulkphase is different with different cavity spacing. The amount of surfactant will dictate the visibility during later stages of the measurements, the decrease in visibility was seen especially during experiments with larger cavity spacing. This problem can be solved e.g. through using more advanced pipettes with a small 'needle' diameter and specifically with adjustable deposition volume. The appropriate ratio between the volume of deposited surfactant and oil bulkphase volume has not been studied but is important for this problem. Additionally only triton X-15 and triton X-15+Triton X-100 surfactants were used in this study and a more detailed study on the variation of surfactant solution would be interesting.

6.2 Fitting data

Surfactant propagation, 0,150mm cavity spacing	a	0,47095	0,09583
	b	0,39542	0,24016
Surfactant propagation, 0,375mm cavity spacing	a	0,52351	0,05776
	b	1,07894	0,30055
Surfactant propagation, 0,600mm cavity spacing	a	0,52992	0,1142
	b	1,26626	0,53834
Surfactant propagation, 0,825mm cavity spacing	a	0,44685	0,04146
	b	2,15061	0,38084
Surfactant propagation, 1,00mm cavity spacing	a	0,53983	0,05673
	b	1,56979	0,34699

Figure 23: Tables showing the fitdata with the different cavity spacing. The fitsheet of the first measurement.

Surfactant propagation, 0,150mm cavity spacing	a	0,36656	0,09903
	b	1,68601	0,72976
Surfactant propagation, 0,375mm cavity spacing	a	0,47195	0,05176
	b	1,30535	0,35485
Surfactant propagation, 0,600mm cavity spacing	a	0,77958	0,07699
	b	0,52695	0,17106
Surfactant propagation, 0,825mm cavity spacing	a	0,44602	0,04343
	b	1,74262	0,34743
Surfactant propagation, 1,00mm cavity spacing	a	1	0,4245
	b	0,1462	0,23737
Surfactant propagation, 2,00mm cavity spacing	a	0,61044	0,10877
	b	0,72784	0,31905

Figure 24: Tables showing the fitdata with the different cavity spacing. The fitsheet of the second measurements.

Surfactant propagation, gap 0,5mm	a	0,40794	0,04355
	b	4,11505	0,56142
Surfactant propagation, gap 1,2mm	a	0,63667	0,04661
	b	0,87427	0,17881
Surfactant propagation, gap 2,6mm	a	0,41136	0,04126
	b	2,2468	0,40951
Surfactant propagation, gap 3mm	a	0,4557	0,06002
	b	2,07447	0,53589

Figure 25: The fitdata of the measurements with varied gap spacing

References

(1) DOE - Fossil Energy: DOE’s Oil Recovery R&D Program
(2) Sigma-Aldrich: Triton X-100 non-ionic detergent
(3) Griffin WC: ’Classification of Surface-Active Agents by ’HLB’, Journal of the Society of Cosmetic Chemists 1 (1949): 311.
(4) Steffen Berg: Structure formation and transport in complex systems, Shell International Exploration & Production B.V.
(5) S. Berg, Phys. Fluids, 2009, 21, 032105.
(6) D. K. N. Sinz and A. A. Darhuber, to be published
(7) Z. Dagan, PCH/PhysicoChemical Hydrodynamics (ISSN 0191-9059), vol. 5, no. 1, 1984, p. 43-51.